METALS AND MATERIALS International, Vol. 7, No. 3 (2001), pp. 251~256

The Effect of Precipitation on the Evolution of Recrystallization Textures in an AA 8011 Aluminum Alloy Sheet

Jong-Ho Ryu, Yoon-Soo Lee* and Dong Nyung Lee

School of Materials Science and Engineering, Seoul National University
56-1 Shinrim-dong, Kwanak-ku, Seoul 151-742, Korea
*Samsung SDI Co., Ltd., 575 Sin-dong, Paldal-ku, Suwon 442-391, Korea

The texture of an AA 8011 aluminum alloy sheet cold rolled by 95% showed a typical β-fiber, which runs from the copper orientation [C={112}<111>] over S [{123}<634>] to brass [B={011}<112>]. The development of annealing textures depended on annealing temperatures due to the interaction between precipitation and recrystallization. Upon annealing at a low temperature of 275°C, precipitation took place before recrystallization. This led to a weak recrystallization texture consisting of {011}<122>, {001}<100>, and {hk0}<001>, among which the {011}<122> orientation developed near large $FeAl_3$ particles as the main orientation and the cube [{001}<100>] orientation originating from the matrix was relatively weak. After annealing at 350 and 500°C, a strong cube texture developed along with a weak {011}<122> orientation. When the cube orientation developed, the copper orientation disappeared most rapidly. These results were discussed based on the interaction between precipitation and recrystallization.

Keywords : AA 8011 aluminum alloy, particle stimulated nucleation, rolling texture, recrystallization texture

1. INTRODUCTION

Both the deformation and recrystallization of metals give rise to the development of characteristic textures, which in turn lead to anisotropic properties. Over forty years much effort has been directed toward defining the critical parameters which control the recrystallized structure of binary aluminum alloys containing dispersions of intermetallic compounds [1-15]. In the annealing of a material containing second phase particles, the interaction between precipitation and recrystallization controls the annealing mechanism. Fig. 1 shows a schematic diagram of the interaction between precipitation and recrystallization suggested by Hornbogen and Köster [16]. According to the figure, recrystallization occurs prior to precipitation at high temperatures, whereas precipitation takes place prior to recrystallization at low temperatures. However, the texture evolution in commercial alloys may be more complicated.

The objective of this study is to investigate the effect of precipitation on the evolution of textures in a 95% cold rolled 8011 aluminum alloy sheet during annealing at different temperatures.

2. EXPERIMENTAL PROCEDURES

An AA 8011 aluminum alloy sheet, which contained 0.71%Fe, 0.65%Si, and 0.034%Ti, was solution-treated at 600°C for 18 h and subsequently quenched in cold water. The solution-treated sheet rotated through 90° about the normal direction, was cold-rolled to 0.32 mm in thickness (95% reduction) through about 50 passes and annealed isothermally at 275, 350, and 500°C in a salt bath.

The electrical conductivity of this material was measured to detect precipitation. The Vickers microhardness measurements were carried out under an indenting load of 50 g on the mechanically polished longitudinal sections of the speci-

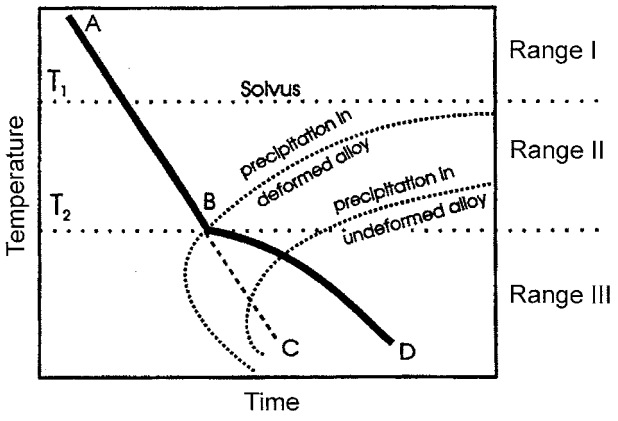

Fig. 1. Schematic diagram showing interaction between precipitation and recrystallization [16].

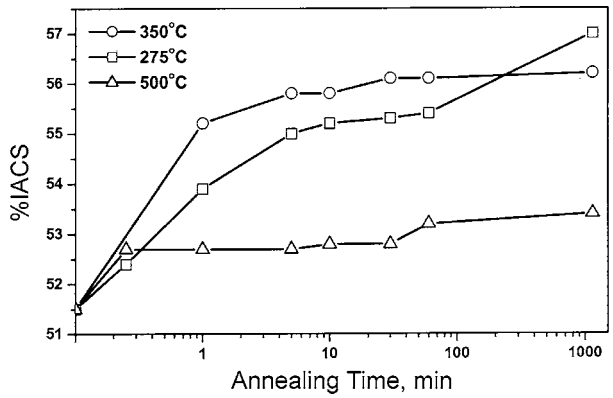

Fig. 2. Electrical conductivity of 95% cold rolled AA 8011 aluminum alloy sheet as a function of annealing temperature and time.

mens. In order to measure textures, incomplete pole figures of (200), (111), and (220) were measured and used to calculate orientation distribution functions (ODFs) by the series expansion method [17]. The ghost correction was made using the positivity method [18]. The deformation zone around precipitates in cold-rolled sheets and the particle stimulated nucleation (PSN) during annealing were observed by TEM.

3. RESULTS

Fig. 2 shows the electrical conductivity of the cold-rolled sheet as a function of annealing time at three different temperatures. The conductivity of the sheet annealed at 500°C almost reached the saturated level within 1min and from this time on slowly increased to about 53% IACS. The conductivity of the sheet annealed at 350°C reached the saturated value of 56% IACS after 30min. The conductivity of the sheet annealed at 275°C increased to 57% IACS after 1140min. As the annealing temperature increases, the precipitation rate increases, which in turn gives rise to a decrease in time to the conductivity saturating level, and the solute solubility increases, resulting in a decrease in the peak conductivity.

Fig. 3(a) shows the texture of the center layer of the solution-treated sheet. The texture was nearly random. Fig. 3(b) shows the texture of the 95% cold-rolled specimen, which is characterized by a typical cold rolling texture (β-fiber texture). The β-fiber texture runs from the copper orientation [C={112}<111>] over the S orientation [{123}<634>] to the brass orientation [B={011}<112>]. The intensity of the C-orientation is similar to that of the S-orientation, while the B-orientation is weaker than the C and S orientations.

When the cold rolled specimen was annealed at 275°C for 1h, its texture remained almost unchanged, though the orientation intensity slightly increased as shown in Fig. 4(a). However, after annealing for 19 h at the same temperature, a marked change in texture took place, as shown in Fig. 4(b). The drop in hardness was observed after annealing at 275°C

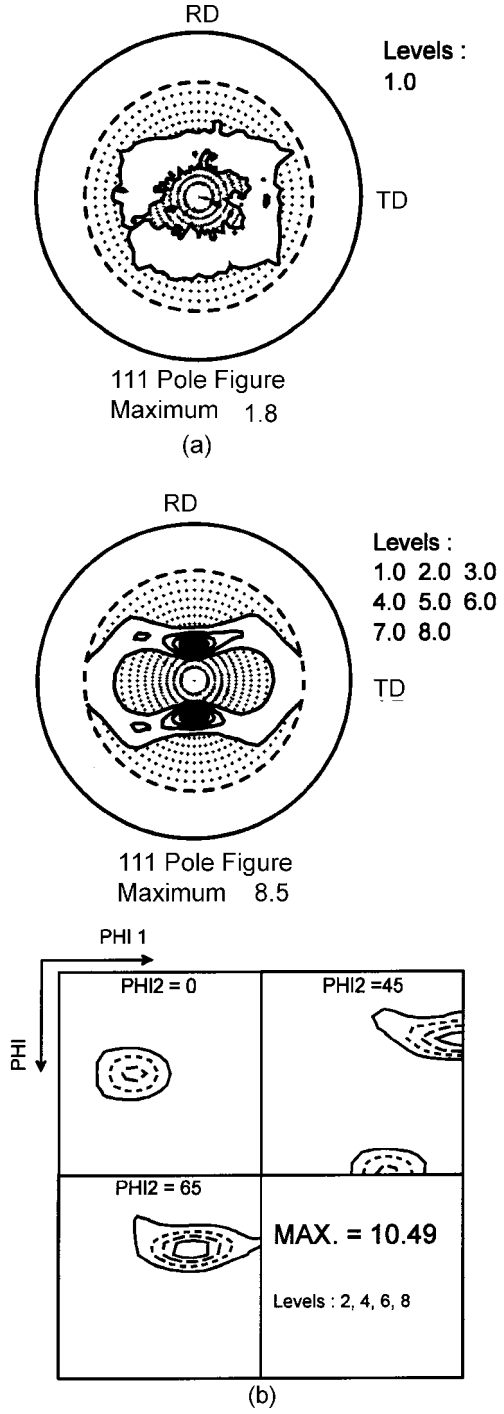

Fig. 3. Textures of AA 8011 aluminum alloy sheet (a) before and (b) after cold rolling by 95%.

for 19h, as shown in Fig. 5. The texture change and the hardness drop indicate that recrystallization occurred even after annealing at 275°C for 19 h. The recrystallization texture shown in Fig. 4(b) consists of the cube orientation [{001}<100>], the P-orientation [{011}<122>], and the RD rotated cube orientation [{hk0}<001>], with the P-orientation a little

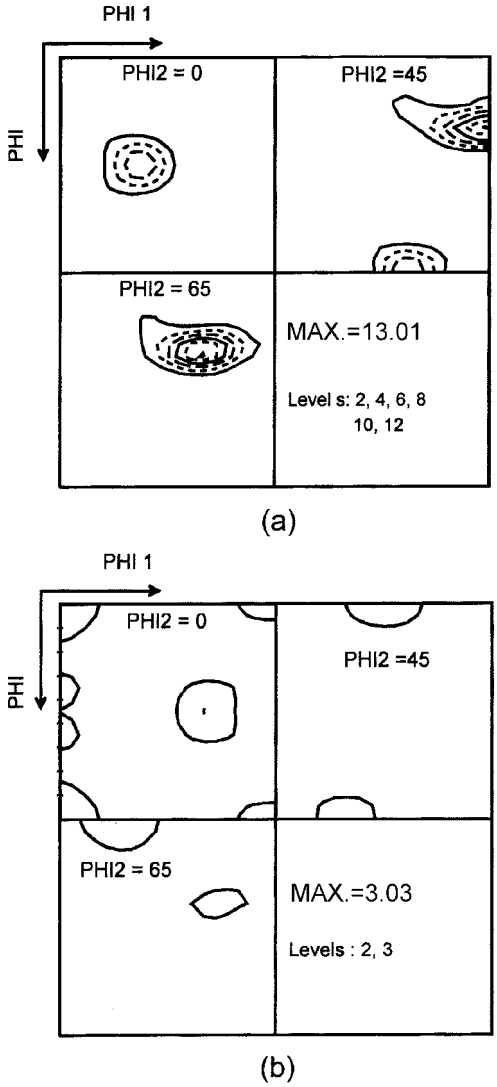

Fig. 4. ODFs of AA 8011 aluminum alloy sheets cold rolled by 95% and annealed at 275°C for (a) 1 h and (b) 19 h.

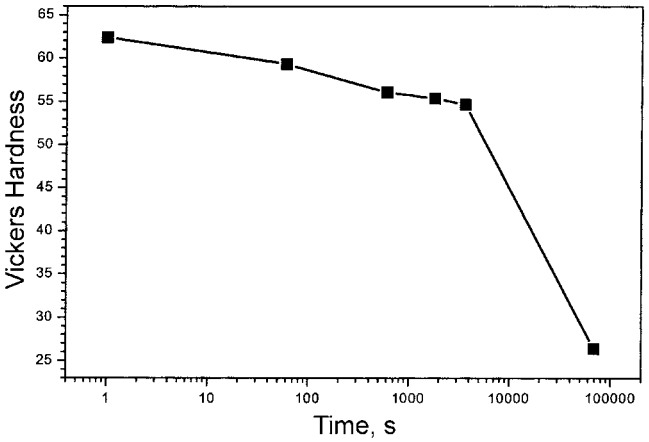

Fig. 5. Hardness of 95% cold rolled AA 8011 aluminum alloy sheet as a function of annealing time at 275°C.

stronger than the cube orientation. It is known that the P-component develops when rolled aluminum alloy sheets including hard particles are annealed [2, 5, 9, 19, 20].

Fig. 6 shows the texture of specimen as a function of annealing time at 350°C after cold rolling by 95%. All the textures were almost the same as were the strong cube and weak P-orientation, implying that recrystallization was completed within 5min at 350°C. It is interesting to note that for the texture obtained at 350°C the cube orientation is much stronger than the P-orientation, unlike the texture obtained at 275°C in which the P-orientation is slightly stronger than the cube orientation. Fig. 6 also shows that when the cube orientation appears, the copper orientation disappears faster than the S and B orientations. Variations of orientation densities of the cube, B, C, and S orientations with annealing time at 350°C are given in Table 1. This implies that the copper orientation is more responsible for the cube orientation than other orientations. Lee [21-23] explained the transformation of the C-orientation into the cube recrystallization texture by the strain energy release maximization model. When annealed at 500°C for 1h, the specimen had the strong cube - weak P texture as shown in Fig. 7.

Fig. 8 shows TEM structures of cold rolled and annealed aluminum alloy specimens. The large particle in the cold rolled specimen was found to be $FeAl_3$ (Fig. 8(a)), indicating that $FeAl_3$ particles did not dissolve during solution treatment at 600°C. Local deformation zones around the large particles, which had a texture different from the β-fiber texture in the matrix, gave rise to the P-orientation after recrystallization as shown in Fig. 8(b). Upon annealing, silicon precipitated as shown in Fig. 8(c), which also shows that dislocations are pinned by silicon precipitates. It is noted that silicon precipitated in a very short time (15 s) at 500°C.

4. DISCUSSION

4.1. Recrystallization at a low temperature

The increase in conductivity of the cold rolled specimen with the increase of annealing time at 275°C is mainly due to precipitation and a minor contribution of recovery up to 60 min (Figs. 2 and 5). A rapid increase in conductivity between annealing times of 60 and 1140 min can be attributed to recrystallization from the hardness data in Fig. 5. The texture change after prolonged annealing at 275°C is attributed to recrystallization (Fig. 4(b)). It follows from the above results that, when the specimen was annealed at 275°C, substantial precipitation took place before recrystallization occurred. This temperature belongs to range III in Fig. 1.

The relatively weak recrystallization texture indicates that recrystallized grains of any particular texture could not grow extensively due to pinning by precipitates. It is known that

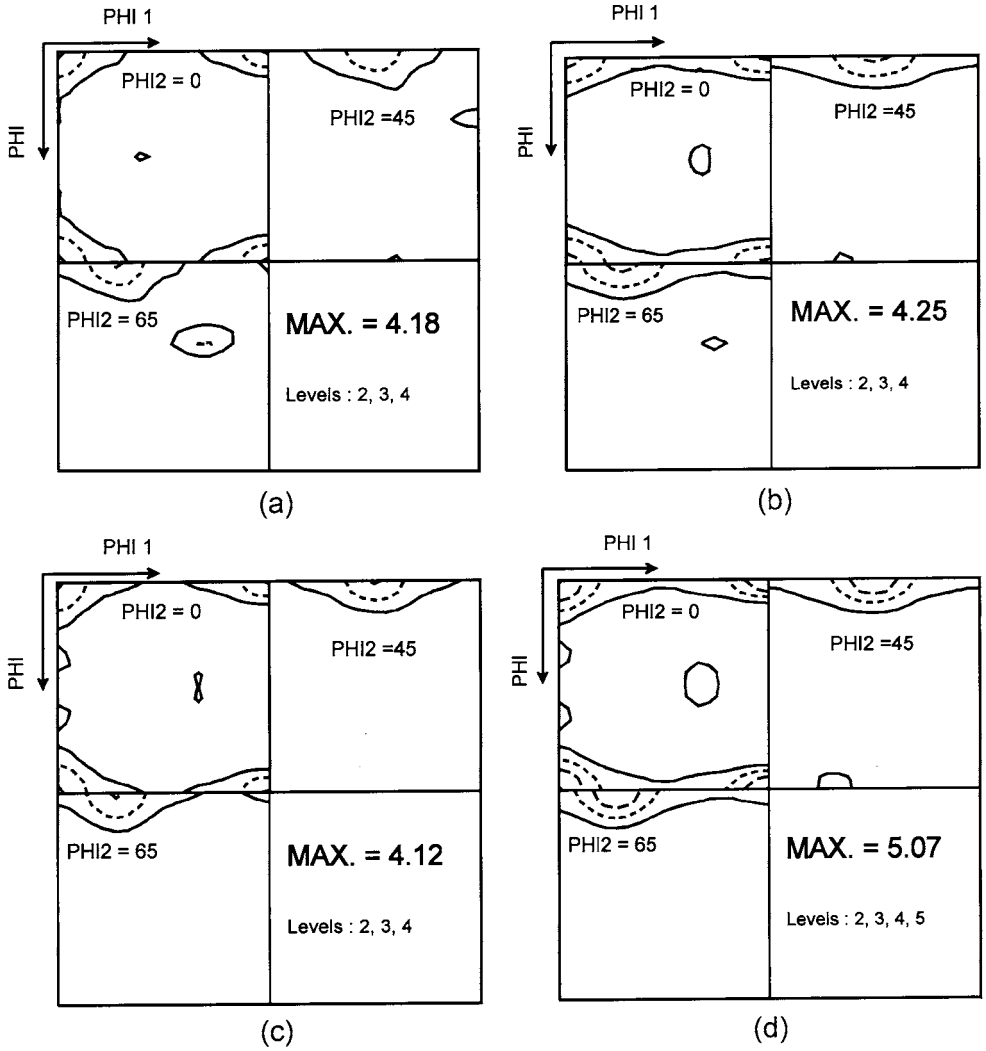

Fig. 6. ODFs of AA 8011 aluminum alloy sheets cold rolled by 95% and annealed at 350°C for (a) 5 min, (b) 30 min, (c) 1h and (d) 19 h.

Table 1. The orientation densities of the cube, B, C, and S orientations after various annealing times at 350°C

	Cube {001}<100>	B {011}<112>	C {112}<111>	S {123}<634>
0 min		6.86	10.47	9.7
5 min	4.18	2.11	2.4	3.0
30 min	4.25		1.3	2.23
60 min	4.12		1.3	1.94
1140 min	5.07		1	1.9

the cube texture develops from copper and aluminum sheets having the β-fiber texture and the P-orientation originates from particle stimulated nucleation. The local strains near hard particles are higher than those in the matrix, which in turn gives rise to a higher driving force for recrystallization near the particles than in the matrix, resulting in the higher intensity of P-orientation.

4.2. Recrystallization at high temperatures

The recrystallization texture developed at 350 and 500°C are characterized by the strong cube and weak P orientations and the texture at 500°C is stronger than that at 350°C. The conductivity data in Fig. 2 indicate that precipitation took place at the start of annealing at 350 and 500°C. Fig. 8(c) shows that silicon precipitated in a very short time (15 s) at 500°C and dislocations were pinned by silicon precipitates. The conductivity of the specimen annealed at 350°C is higher than that at 500°C because the solid solubility at 350°C is lower than that at 500°C. The strong cube and weak P texture indicates that recrystallization occurred in the matrix as well as near the $FeAl_3$ particles almost simultaneously and the volume of the matrix was larger than that of the deformation zone near the particles whose texture differed from the β-fiber texture in the matrix.

According to Fig. 1, for the specimen annealed at 350 and 500°C, precipitation must not have taken place before recrys-

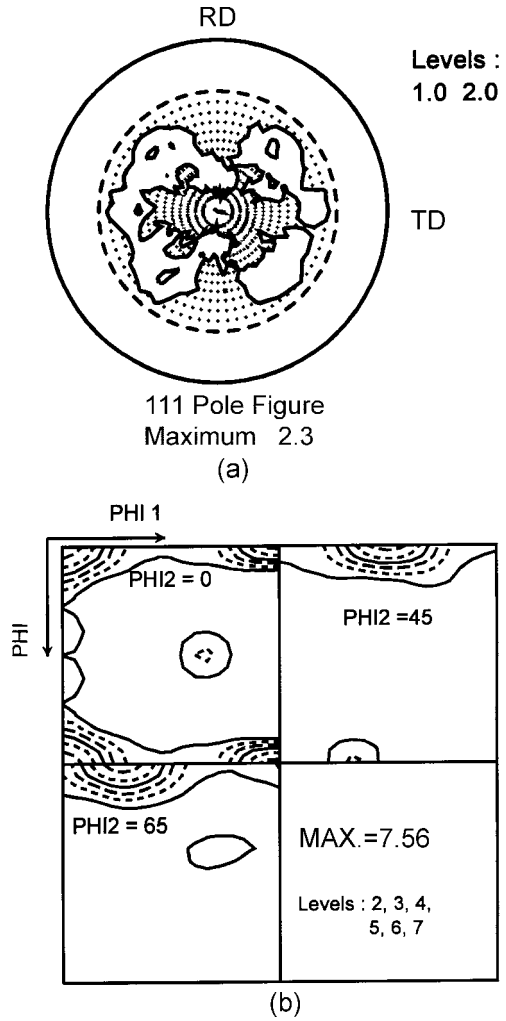

Fig. 7. (a) (111) pole figure and (b) ODF of AA 8011 aluminum alloy sheet cold rolled by 95% and annealed at 500°C for 1h.

tallization occurred because the temperatures of 350 and 500°C belong to range II. However, precipitation took place at the start of annealing at 350 and 500°C as discussed above. Therefore, the interaction in Fig. 1 cannot apply to the annealing behavior at 350 and 500°C.

At the high temperatures of 350 and 500°C, the driving force for recrystallization can be interpreted to be higher than the dragging force of precipitates. The stronger texture development at 500°C than at 350°C can be attributed to a higher driving force and fewer precipitates at the higher temperature.

5. CONCLUSIONS

1. The texture of an AA 8011 aluminum alloy sheet cold rolled by 95% was a typical β-fiber with high densities in the C and S orientations.

2. Its annealing texture depended on its annealing temperature due to the interaction between precipitation and recrystallization. Upon annealing at a low temperature of 275°C, precipitation took place before recrystallization. This resulted in a weak recrystallization texture consisting of {011}<122>, {001}<100>, and an RD rotated cube [{hk0}<001>], among which the strong {011}<122> orientation formed near the large $FeAl_3$ particles was the main texture and the {001}<100> orientation originated from the matrix was relatively weak.

3. On annealing at 350 and 500°C, the {001}<100> orientation developed strongly, while the {011}<122> orientation was weak, because the driving force for the recrystallization of the matrix was higher than the dragging force of the precipitates.

4. When the {001}<100> orientation appeared, the {112}<111> orientation disappeared most rapidly. This can imply that the copper deformation texture is more responsible for the cube recrystallization texture than other orientations. This

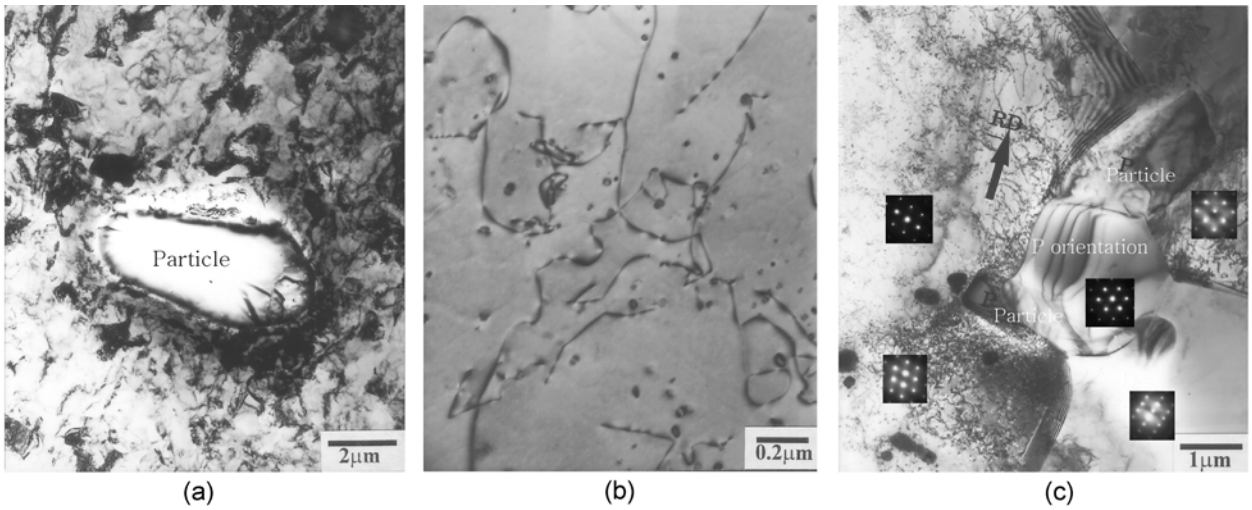

Fig. 8. Transmission electron micrographs showing (a) one $FeAl_3$ particle in 95% cold rolled AA 8011 aluminum alloy sheet, (b) {011}<122> oriented grain between $FeAl_3$ particles and (c) silicon precipitates in AA 8011 aluminum alloy sheet cold rolled by 95% and annealed at 500°C for 15 s.

result is compatible with the prediction of the strain energy release maximization model.

ACKNOWLEDGMENT

This study has been supported by the National Research Laboratory for Texture Control, Seoul National University.

REFERENCES

1. E. Nes and J. D. Embury, *Z. Metallkd*. **66**, 589 (1975).
2. S. Benum and E. Nes, *Acta mater*. **45**, 4593 (1997).
3. K. Ito, K. Lücke and R. Rixen, *Z. Metallkd*. **67**, 338 (1976).
4. K. Ito, R. Musika and K. Lücke, *Acta metall*. **31**, 2137 (1983).
5. O. Engler, X. W. Kong and P. Yang, *Scripta mater*. **37**, 1665 (1997).
6. F. J. Humphreys, *Proc. ICOTOM 11*, p. 1191, Xian, China (1996).
7. C. P. Johnson and F. J. Humphreys, *Proc. ICOTOM 11*, p. 1263, Xian, China (1996).
8. H. M. Chan and F. J. Humphreys, *Acta metall*. **32**, 235 (1984).
9. H. E. Vatne, O. Engler and E. Nes, *Mater. Sci. Tech.* **13**, 93 (1997).
10. D. J. Jensen, N. Hansen and F. J. Humphreys, *Acta metall*. **33**, 2155 (1985).
11. F. Habiby and F. J. Humphreys, *Textures and Microstructures* **20**, 125 (1993).
12. I. Samajdar, L. Rabet, B. Verlinden and P. Van Houtte, *ISIJ Int*. **38**, 539 (1998).
13. J. Hjenlen, R. Ørsund and E. Nes, *Acta metall. mater*. **39**, 1377 (1991).
14. H. Weiland, T. N. Rouns and J. Liu, *Z. Metallkd*. **85**, 592 (1994).
15. O. Engler, *Mater. Sci. Tech*. **12**, 859 (1996).
16. E. Hornbogen and U. Köster, *Recrystallization of Metallic Materials* (ed., F. Haessner), p. 159, Riederer Verlag GmbH, Stuttgart (1978).
17. H. J. Bunge, *Mathematische Methoden der Texturanalyse*, Akademie-Verlag, Berlin (1969).
18. F. Wagner and M. Dahms, *Advances and Applications of Quantitative Texture Analysis* (eds., H. J. Bunge and C. Esling), Informationsgesellschaft mbH, Oberursel (1991).
19. O. Daaland and E. Nes, A*cta mater*. **44**, 1413 (1996).
20. K. Lücke and O. Engler, *Mater. Sci. Tech.* **6**, 1113 (1990).
21. D. N. Lee, *Scripta metall.* **32**, 1689 (1995).
22. D. N. Lee, *Metals and Materials* **5**, 401 (1999).
23. D. N. Lee, *Int. J. Mech. Sci.* **42**, 1645 (2000).